Application of advanced fluorescence microscopy to the structure of meiotic chromosomes

Peter M. Carlton

Institute for Integrated Cell-Material Sciences (WPI-iCeMS), Kyoto University

Phone: 81 75 753 9853

pcarlton@icems.kyoto-u.ac.jp

www.carlton.icems.kyoto-u.ac.jp

Keywords: meiosis, synaptonemal complex, superresolution microscopy, 3D-SIM

Abbreviations: SC, synaptonemal complex; CE, central elements; LE, lateral elements

Abstract:

Chromosomes undergoing meiosis are defined by a macromolecular protein assembly called the synaptonemal complex, which holds homologs together and carries out important meiotic functions. By retaining the molecular specificity, multiplexing ability, and *in situ* imaging capabilities of fluorescence microscopy, but with vastly increased resolution, 3D-SIM and other superresolution techniques are poised to make significant discoveries about the structure and function of the synaptonemal complex. This review discusses recent developments in this field and open questions approachable with current and future technology.

Visualizing subcellular structures beyond the diffraction limit

Significant technical advances in microscope resolution have occurred in recent years. Precision control of excitation light and fluorophore characteristics, combined with computational techniques for reconstructing image information from raw data, have enabled the development of several superresolution imaging modalities (Schermelleh et al., 2010) capable of resolving objects more finely than the Abbe diffraction limit. One superresolution technique, three-dimensional structured illumination microscopy (3D-SIM) (Gustafsson et al., 2008; Schermelleh et al., 2008) enables enhancement of resolution by a factor of two in both the lateral and axial directions, to 100nm in XY and 250nm in Z. Because of its resolution range, 3D-SIM is most effectively applied in visualizing subcellular structures that fall between 100 and 200nm. Meiotic chromosomes in particular are attractive targets for 3D-SIM (Carlton, 2008) due to several of their structural features.

Meiosis and the Synaptonemal Complex

Sexually reproducing organisms create their gametes through meiosis, a series of two cell divisions which partition a diploid genome between two haploid daughter cells, each obtaining a complementary half of the genetic material. This precise partitioning is accomplished by the *de novo* pairing of homologous chromosomes before their segregation, followed by the establishment of exchanges between homologs that orient them in opposite directions at metaphase I. Meiotic chromosomes appear as long, thin threads, separately distinguishable yet not as condensed as during the mitotic cell cycle. It has long been hypothesized that this striking appearance, and its underlying structural basis, reflect functional requirements.

A near-universal structural component of meiotic chromosomes is the synaptonemal complex (SC), a zipper-like protein macroassembly that localizes between paired homologous chromosomes along their lengths (reviewed extensively in Zickler & Kleckner, 1999). The SC is composed of two major parts. The first is a protein core that extends the length of each individual chromosome; the cores are referred to as axial elements (AE) before the intimate association (synapsis) of chromosomes, and as lateral elements (LEs) afterwards. The second part is the central element (CE), a zipper-like structure that polymerizes between opposed AEs when homologous chromosomes synapse (**Figure 1**). The SC plays key roles in enabling chromosome pairing and recombination, is necessary for proper chromosome morphology, and likely has additional roles in control of recombination (Hayashi et al., 2010). Any defects in SC formation are likely to disrupt proper gamete formation, causing sterility. Thus, the formation and disassembly of the SC are under strict regulation.

The SC was first discovered over 50 years ago by electron microscopy (EM) studies of meiotic chromosomes (Moses, 1956; Fawcett, 1956). EM images revealed the basic dimensions of the complete SC: LEs are spaced from 100-200nm apart, and CE filaments (the "teeth" of the zipper) are spaced roughly 20-30nm apart (**Figure 2**). The ability to reconstruct entire SC complements of meiotic cells from serial-sectioned EM images was a significant advance in cytogenetics, as the paths of synapsed and unsynapsed chromosomes could be seen in their entirety in situ. However, the nature of the SC itself remained mysterious, until its molecular components could be identified. We now know the SC is composed of many different proteins, interlocking in a complicated mesoscale polymer framework. Protein components of both LEs and CEs have been identified in animals, fungi, and plants (**Table 1**). CE components include the transverse filaments (Solari & Moses, 1973), coiled-coil proteins that extend from the LEs to meet at the center, as well as other proteins that localize to the central region (Bolcun-Filas et al., 2007; Fraune et al., 2012; Page et al., 2008). LE components include SC-specific proteins, including many proteins with HORMA domains (Aravind & Koonin, 1998; Couteau et al., 2004) as well as cohesin proteins that make up the axial core (Eijpe et al., 2003). One of the most comprehensive recent studies of SC structure has been performed in the nematode *Caenorhabditis elegans*, using a combination of

genetic, biochemical, and immuno-electron microscopy image data of the CE (Schild-Prüfert et al., 2011). The resulting model is likely the most detailed yet provided in any organism, and defines which of the known CE proteins of *C. elegans* (SYP-1, -2, -3, and -4) make direct contact with each other at which end (N- or C-terminus). The actual structure or structures that satisfy the constraints provided by this consensus model, as well as their higher-order organization within the SC, remain to be elucidated. While the SC is grossly similar between different species, considerable variation exists in protein makeup, connectivity and overall architecture (reviewed in Hawley, 2011).

Like most biological structures, the SC is capable of dynamic reorganization and modification, including assembly, disassembly, and covalent modification of specific subunits, e.g., through phosphorylation (Bailis & Roeder, 1998; Fukuda et al., 2012) or SUMOylation (Watts & Hoffmann, 2011). However, while biochemical and genetic studies have greatly increased our knowledge of the components that make up the SC, a complete structural and functional explanation, including how it interfaces with meiotic chromatin, remains elusive. Part of the difficulty has arisen from the fact that the dimensions of the SC lie below the diffraction limit of visible light (250-350nm), rendering optical microscopy relatively ineffective as a tool to reveal its detailed composition. Recently, new forms of superresolution microscopy have begun to be successfully applied to the study of the SC, bridging the gap between the molecular specificity of fluorescence microscopy and the high resolution required for structural information to be uncovered.

3D-SIM applied to meiotic chromosomes

3D-SIM has been successfully used to observe meiotic chromosomes in plant and animal meiosis. (Wang et al., 2009) used immunostaining of AFD1, a homolog of kleisin Rec8, to demonstrate 3D-SIM's ability to optically resolve both LEs in maize. The spacing of AFD1 was measured at 190nm, consistent with previous EM studies of total SC width (Gillies, 1973). Additional structural details of the SC, such as its coiling (see below) and the resolution of entanglements, were also quantitatively measured. In a recent study, Phillips et al. (Phillips et al., 2012) examined the SCs of barley with 3D-SIM, examining not only the LE HORMA-domain protein ASY1 (Armstrong et al., 2002) but also ZYP1, a transverse filament protein (Higgins et al., 2005). By simultaneously viewing both proteins with 3D-SIM, they were able to discern two different types of SC structure coexisting in the same nucleus. In addition to a canonical tripartite structure, where LEs and CEs lie in the same plane, they also discovered a two-level organization of ZYP-1 both above and below the LE plane (**Figure 2C**). The authors performed immunostaining with antibodies raised against ZYP1's C-terminus, which localizes near the LEs. 3D-SIM was sufficient to show that ZYP1 localized internally to ASY1, demonstrating its ability to quantitatively measure substructures within the SC. It will be interesting to determine whether the observed variation between the two SC structures has any functional consequence. In animal systems, genetic

studies have added further information to what can be inferred by cytology. (Qiao et al., 2012) used 3D-SIM to examine the SCs of mouse chromosomes. Their cytological data provided evidence for new roles of the CE transverse filament protein Sycp1 in regulating exchanges between LEs at crossover sites and preventing unregulated axis associations. With the higher resolution of 3D-SIM it was also apparent that centromeric ends of LEs displayed malformations in the absence of Sycp1. In *C. elegans*, (Zhang et al., 2012) employed 3D-SIM to investigate the localization of CE transverse filament protein SYP-1 (MacQueen et al., 2002) in wild-type animals and in a strain carrying a mutation (*hal-2*) which prevents homologous pairing. In nuclei missing the HAL-2 protein, CE proteins abnormally loaded onto single, unsynapsed LEs (detected with immunostaining against HTP-3, one of four HORMA domain-containing proteins in the *C. elegans* LE). The LEs in *hal-2* mutants appeared as single tracks by 3D-SIM, in contrast to wild-type animals in which 3D-SIM can resolve both LE tracks. In the above examples, 3D-SIM microscopy enabled quantitative measurements of 3D higher-order structural details of specific protein molecules, a significant improvement over previous forms of microscopy.

4pi microscopy applied to meiotic chromosomes

Another superresolution modality recently applied to the study of meiotic chromosomes is 4pi microscopy (Schrader et al., 1998). 4pi microscopy uses two objective lenses to capture emitted fluorescence from both sides of the sample, increasing the axial resolution by a factor of from 2-7, down to ~80 nanometers. Since the axial resolution of conventional microscopy is so poor (500-700nm), it is often a limiting factor in the interpretation of cell image data. In the case of the SC, two paths that may be distinguishable in the XY plane can merge into ambiguity when viewed from the side. With 4pi microscopy, however, Fritsche et al. were able to trace the paths of mouse SCs with extremely high accuracy, and incorporate this data into a physical model of large-scale chromosome organization. This example highlights the utility of superresolution not only for obtaining sub-diffraction structural data, but also for overcoming long-standing barriers to quantitative imaging associated with limited-resolution systems.

Other super-resolution techniques applicable to meiotic chromosomes

Higher resolution with localization microscopy and STED

Although 3D-SIM and 4pi microscopy offer great improvements over conventional widefield imaging, the dimensions of the SC as seen by EM (around 100nm) can lie near or past the limit of their resolution capabilities. Especially when using longer

wavelengths of light, the resolution of 3D-SIM may be insufficient to resolve LEs or transverse filament proteins as two-track structures. Additionally, since the axial resolution of 3D-SIM is still limited to c. 250nm, only a subset of views of the SC within a sample are amenable to 3D-SIM analysis. To achieve even more detailed views of the SC, it will be necessary to make use of higher-resolution imaging techniques. Two promising techniques for continued studies of the SC are (1) single-molecule localization microscopy, also known as (F)PALM or STORM, and (2) STED microscopy (both reviewed in Toomre & Bewersdorf, 2010).

Localization microscopy can achieve tremendous resolution, on the order of 20-50nm, in both the lateral and axial directions. By imaging the individual positions of a large number of stochastically activated single molecules within a structure, and fitting a mathematical distribution to the image data, the molecules' positions in space can be localized to a very high precision. Axial (Z) information may be obtained via several enhancements to the basic technique, such as the use of astigmatism (Huang et al., 2008), simultaneous recording of several focal planes (Juette et al., 2008), or, in the iPALM technique, exploiting the interference in emitted photons passing through opposing objective lenses (Shtengel et al., 2009). The precision of localization is limited in principle only by the number of photons that can be detected above the background level. Recent advances in chemical fluorophore modification have provided further improvements in probe brightness, potentially allowing localization to just several nanometers (Vaughan et al., 2012). Localization microscopy can be performed with several probes simultaneously, making it a strong technique for exploring the structural composition of the SC in three dimensions.

STED microscopy is a superresolution extension of confocal scanning microscopy. It achieves superresolution by adding a shaped fluorescence-depleting beam to the normal excitation beam. The depletion beam shrinks the effective size of the excitation spot to below the diffraction limit, theoretically as small as desired but practically limited to the same range as localization microscopy, 50±30 nm. STED and 4pi microscopy can be combined to enable isotropic multi-wavelength resolution of ~30nm in both the lateral and axial directions (Schmidt et al., 2009). Multicolor 4pi-STED could potentially acquire images of the SC on the same size scale as localization microscopy. As the resolution of these techniques approaches and may surpass the ~20-30nm spacing of transverse filaments seen in many EM preparations (Schmekel et al., 1993), they have incredible potential to unlock the remaining structural ambiguities of the SC.

Unanswered questions about SC structure

Chromatin accommodation within the SC

Before synapsis can occur, AEs must be properly formed in close association with chromatin. Surprisingly little is known about the mechanism of forming early meiotic prophase chromosomes. Meiotic chromosomes before synapsis consist of loops of chromatin bound to a cohesin core (Moens & Pearlman, 1988). The

spacing of loops is relatively constant between species, covering a range from 15 to 45 loops per μm (Kleckner, 2006). ChIP experiments have discovered chromosome locations that are reproducibly enriched for axial associations (Blat & Kleckner, 1999; Glynn et al., 2004) in yeast. These sites represent a population consensus; actual loop formation sites in any given cell are likely somewhat variable. The proteins that make up the chromosome axis include the cohesin family (Eijpe et al., 2003). With the discovery of Rad21L (Ishiguro et al., 2011; Lee & Hirano, 2011), it was also shown that the order of different cohesins along the meiotic chromosome was largely mirrored between homologs, even before synapsis. It should be possible to further elucidate this heterogeneity in SC structure with higher-resolution imaging studies.

The chromatin loops themselves may present an underappreciated barrier to synapsis. It has been suggested that if chromatin loop sizes are large compared to their spacing, then the loops would surround the axial element with a halo of chromatin, as a result of the loops' tendency to assume an equilibrium conformation (Marko & Siggia, 1997). For two AEs to synapse, approaching within less than 200nm of each other, this halo of chromatin must be displaced; i.e., the chromatin located between the AEs must somehow move out of the way. If the properties of the chromatin do not otherwise change at this time, this displacement would cause an increase in the density of chromatin loops, which would be resisted by "chromatin pressure", a manifestation of the chromatin fiber's tendency to resume its equilibrium conformation. A feature common to meiotic chromosomes at this stage of initial pairing is rapid dynamic movement of chromosome ends mediated by the cytoskeleton (Baudrimont et al., 2010; Chikashige et al., 2009; Koszul et al., 2008; Morimoto et al., 2012; Wynne et al., 2012); it is conceivable that this movement could provide some of the necessary force to make axes coincide. Alternatively, several observations of chromosomes before and after synapsis suggest that instead of a radial arrangement, the loops of chromatin point away from the axis, as co-oriented arrays (reviewed in Kleckner et al., 2004). This arrangement, which could conceivably be brought about by specific interactions between chromatin and the axis, would be more favorable to pairing.

Twisting of the synaptonemal complex

Twisting as a general feature of SC structure has been known from EM reconstructions from serial sections (see e.g. (Lin, 1979)). Using 3D-SIM, Wang et al. observed SC twisting in maize, with a strong bias toward left-handed helicity. Phillips et al. also observed twisting in their preparations of barley SCs, though without a pronounced handedness bias. The mechanism behind twisting is not known, but the progressive nature of twisting in maize as well as the handedness bias seen in some organisms indicates it may be the result of an active process, and not simply a random or equilibrium configuration. Among the mechanisms that could result in twisting is differential length change: if one part of the meiotic chromosome (the central element, for example) were to contract relative to another part, then twisting could be induced if LE components had a strong tendency to

maintain a constant relative spacing (**Figure 4**). The amount of length contraction necessary would be quite small: given the relation of helix extension z to path length s, $z = \frac{sc}{\sqrt{r^2 + c^2}}$, and the SC's helix radius r (100nm), a length contraction of only 1% would suffice to give a visible half-gyre spacing c of ~2.5µm. A hypothesized relationship of SC twisting to differential lengths of SC components is predicated upon the prevalence of twists in situations of heterologous synapsis, for example differently-sized sex chromosomes (Solari, 1992) or a resizing inversion loop (Moses et al., 1982). Alternatively, twisting may be induced by dynamic movement of chromosome ends at the nuclear envelope (Hiraoka & Dernburg, 2009), if there were any net rotation of chromosome ends in addition to the translational movement. Contrasting synapsis in species with and without biased twisting using super-resolution microscopy may shed light on the mechanisms involved.

Dynamic behavior of the synaptonemal complex

Even less well understood than the SC's structure is the question of its dynamics: how it is assembled, what its behavior is when fully formed, and how it is disassembled. SC initiation is not random: in budding yeast, it initiates at sites bound by the synapsis initiation complex (SIC), which includes proteins Zip2, Zip3, and Zip4. (Fung et al., 2004; Rockmill et al., 1995). The progression of synapsis after initiation has been presumed to be mostly processive, lacking significant desynapsis, in the normal meiotic program. However, this model awaits direct confirmation by *in vivo* observation of synapsis. Little is known about the dynamics of the complete SC. That the SC must be able to dynamically change is inferred by several observations, e.g. (1) Adjustment of inversion loops or deletions (Moses & Poorman, 1981; Poorman et al., 1981; Tease & Fisher, 1986); (2) Correction of synapsis in polyploids from groups of 3 or 4 to pairs of two (Rasmussen, 1977; Rasmussen & Holm, 1979); (3) Extensive desynapsis and resynapsis in response to ionizing radiation (Couteau & Zetka, 2011). Additionally, a recent study in budding yeast, in which a fluorescent Zip1 protein was expressed in prophase-arrested cells with complete synapsis (Voelkel-Meiman et al., 2012) found that new Zip1p molecules continually accumulate in the mature SC, indicating a dynamic flexibility in SC protein stoichiometry. Whether accumulated Zip1p molecules pack into an existing structure, or assume an alternate configuration, remains to be determined. Superresolution imaging of transverse filament molecules that have been differentially labeled could shed light on this question.

Further questions

While we understand SC structure and function in broad outline, several outstanding questions still have only rudimentary answers.

1. What is the stoichiometry and precise position of the various CE proteins in a given sub-assembly, and how do these vary over the length of the SC?

2. Do variant CE substructures have functional differences?

3. What is the higher-order 3D orientation of each sub-assembly? Various possibilities are: subcomplexes always arrange in a polar fashion (i.e., all oriented the same way); always lining up head-to-head and thus without any overall large-scale polarity; or randomly oriented, exhibiting short domains of different polarity over varying lengths.

4. How are the various LE proteins arranged with respect to each other? Several different LE proteins are known to exist, including 4 in *C. elegans*. Whether these form a regularly patterned structure, or separate continuous axes, is not known.

5. How is meiotic chromatin incorporated within the axis? If loops are constrained to point away from the AE, rather than surrounding it, how is this achieved?

In all cases, superresolution optical techniques will be essential tools for obtaining information necessary to answer these questions. Combined with molecular and genetic tools for understanding the functional roles of its protein subunits, the near future will likely see a continued unraveling of the puzzle of how the structure of the SC allows it to carry out such diverse and essential functions in meiosis.

Figure legends

Figure 1: **A**, formation of the SC. Arrows indicate chronological sequence, beginning at upper left. (1) Chromatin loops begin assembling together with axial element proteins, forming loop domains. (2) Continued assembly forms the characteristic leptotene chromosome morphology. (3) Synapsis begins as axes continue to form. Chromatin is excluded from the interface between the two axial elements. (4) Completed synapsis; LEs and CEs form regular, railroad-track-like axis throughout the length of the paired homologs. Inset shows one model of the arrangement of various components.

B, Visualization of *C. elegans* meiotic chromosomes with 3D-SIM microscopy. Chromatin (stained with DAPI), the transverse filament protein SYP-1, and the axial element protein HTP-3, are displayed. For comparison, the image at far right shows the axial elements under conventional deconvolution microscopy. Scale bars, 0.5 μm.

C, Left, highlight of a single optical section (125nm thick) from a meiotic nucleus, showing the two LEs in cross-section in three locations (boxed inset). Right, the entire nucleus in projection, displaying the DNA stained blue, the LEs (HTP-3 protein) stained red, with LEs from the highlighted section shown in yellow. Scale bars, 0.5 μm.

D, 3D-SIM images of cross-sections of *C. elegans* chromosomes, showing axial element protein HTP-3 (yellow), transverse filament protein SYP-1 (blue), and DAPI (gray). Left, the cross-sections

highlighted in the nucleus above. Right, a montage of cross-sections from several nuclei, showing various arrangements of chromatin: either surrounding the entire axis to various extents, or completely bilobed (arrow). Scale bars, 0.5µm.

Figure 2:

A. Before synapsis, homologous chromosomes consist of chromatin loops (violet, gray) attached to an axial core. The size and extent of individual loops are not well-characterized. To allow synapsis, the loops of chromatin must somehow become oriented to allow intimate synapsis at a distance of <200nm.

B. When chromosomes have synapsed, chromatin is often visible as more densely packed and pushed to either side. The central element proteins polymerized between the axes are shown in one possible conformation consistent with the model in (Schild-Prüfert et al., 2011).

C. Schematic of the two kinds of SC structure in barley visualized with 3D-SIM in Phillips et al. (2012). Models of alternate SC structure taken from Phillips et al., 2012. In barley meiocytes, SC was observed by 3D-SIM to exist both in a canonical one-level configuration (right) as well as a two-level configuration (left).

Figure 3: **A**, Relationship between contraction of the center filament (cyan) of an SC-like tripartite ribbon and twisting in the outer axes (red) if they are unable to contract (i.e., if their arc length is constant). In this example simulation, with a radius set to 100nm, and original length of 25µm, a 1% contraction in CE length (arrow) results in ~5.6 full LE twists, ~4.4µm apart. The original position of the right end is indicated by a green line. A full movie of this simulation is shown in the Supplemental data. **B**, 3D-SIM image of a mouse pachytene SC stained with antibodies against Sycp3. Twisting is apparent at a pitch of ~2µm per full turn. Scalebar, 0.5µm.

Table 1. A partial list of synaptonemal complex proteins

	Transverse Filament (TF)	**Central Element (CE)**	**Lateral Element (LE)**	**Cohesin core**
Yeast	ZIP1	Zip2 Zip3 Zip4	Hop1 Mek1 Red1	Rec8
Drosophila	C(3)G	Cona	C(2)M	ORD
C. elegans	SYP-1	SYP-2 SYP-3 SYP-4	HIM-3 HTP-1/2 HTP-3	Rec8
Mouse	SYCP1	Tex12 Syce1 Syce2 Syce3	Sycp2 Sycp3	Rec8

Arabidopsis	ZYP1	Asy1 Asy2 Asy3	SYN1

Supplemental Movie 1: (Nucleus).

The nucleus from **Figure 1C** in maximum-intensity projection. DAPI staining of DNA is shown in blue; the lateral elements stained with anti-HTP-3 in red; and a single section of LE staining is highlighted in yellow. Scale bar, 0.5μm.

Supplemental Movie 2: (Movie of twisting).

A frame-by-frame animation of the twisting as shown in Figure 3. In this movie, contraction of the central element (cyan) begins at the midpoint and proceeds simultaneously to both ends, to a final value of 1% total contraction. Source code in the Processing language is available at: https://github.com/pmcarlton/Chromosomics.

Conflict of interest: None

Acknowledgements:

The author thanks Aya Sato for discussion and critical comments on the manuscript, and Shinichiro Chuma for the mouse spermatocyte sample and anti-Sycp3 antibodies. This work was supported in part by a JSPS Grant-in-Aid for Young Scientists *A* (#24687024). The iCeMS is supported by World Premier International Research Center Initiative (WPI), MEXT, Japan.

References:

Aravind, L. and Koonin, E. V. (1998). The HORMA domain: a common structural denominator in mitotic checkpoints, chromosome synapsis and DNA repair. *Trends in Biochemical Sciences, 23*(8), 284 - 286.

Armstrong, S. J., Caryl, A. P., Jones, G. H., and Franklin, F. C. H. (2002). Asy1, a protein required for meiotic chromosome synapsis, localizes to axis-associated chromatin in Arabidopsis and Brassica. *Journal of Cell Science, 115*(18), 3645-3655.

Bailis, J. M. and Roeder, G. S. (1998). Synaptonemal complex morphogenesis and sister-chromatid cohesion require Mek1-dependent phosphorylation of a meiotic chromosomal protein. *Genes ¥& development, 12*(22), 3551–3563.

Baudrimont, A., Penkner, A., Woglar, A., Machacek, T., Wegrostek, C., Gloggnitzer, J., Fridkin, A., Klein, F., Gruenbaum, Y., Pasierbek, P., and Jantsch, V. (2010). Leptotene/zygotene chromosome movement via the SUN/KASH protein bridge in Caenorhabditis elegans. *PLoS Genet, 6*(11), e1001219.

Blat, Y. and Kleckner, N. (1999). Cohesins bind to preferential sites along yeast chromosome III, with differential regulation along arms versus the centric region. *Cell, 98*(2), 249–259.

Bolcun-Filas, E., Costa, Y., Speed, R., Taggart, M., Benavente, R., De Rooij, D. G., and Cooke, H. J. (2007, Mar). SYCE2 is required for synaptonemal complex assembly, double strand break repair, and homologous recombination. *J Cell Biol, 176*(6), 741-7.

Carlton, P. M. (2008). Three-dimensional structured illumination microscopy and its application to chromosome structure. *Chromosome Res, 16*(3), 351–365.

Chikashige, Y., Yamane, M., Okamasa, K., Tsutsumi, C., Kojidani, T., Sato, M., Haraguchi, T., and Hiraoka, Y. (2009). Membrane proteins Bqt3 and -4 anchor telomeres to the nuclear envelope to ensure chromosomal bouquet formation. *J Cell Biol, 187*(3), 413-27.

Couteau, F., Goodyer, W., and Zetka, M. (2004). Finding and Keeping Your Partner during Meiosis. *Cell Cycle, 3*(8), 1012–1014.

Couteau, F. and Zetka, M. (2011). DNA Damage during Meiosis Induces Chromatin Remodeling and Synaptonemal Complex Disassembly. *Dev Cell, 20*(3), 353-363.

Eijpe, M., Offenberg, H., Jessberger, R., Revenkova, E., and Heyting, C. (2003). Meiotic cohesin REC8 marks the axial elements of rat synaptonemal complexes before cohesins SMC1$¥beta$ and SMC3. *The Journal of cell biology, 160*(5), 657–670.

Fawcett, D. W. (1956). The fine structure of chromosomes in the meiotic prophase of vertebrate spermatocytes. *J Biophys Biochem Cytol, 2*(4), 403–406.

Fraune, J., Schramm, S., Alsheimer, M., and Benavente, R. (2012). The mammalian synaptonemal complex: protein components, assembly and role in meiotic recombination. *Exp Cell Res, 318*(12), 1340–1346.

Fukuda, T., Pratto, F., Schimenti, J. C., Turner, J. M. A., Camerini-Otero, R. D., and Höög, C. (2012). Phosphorylation of chromosome core components may serve as axis marks for the status of chromosomal events during mammalian meiosis. *PLoS Genet, 8*(2), e1002485.

Fung, J. C., Rockmill, B., Odell, M., and Roeder, G. S. (2004). Imposition of crossover interference through the nonrandom distribution of synapsis initiation complexes. *Cell, 116*(6), 795–802.

Gillies, C. (1973). Ultrastructural analysis of maize pachytene karyotypes by three dimensional reconstruction of the synaptonemal complexes. *Chromosoma, 43*(2), 145–176.

Glynn, E. F., Megee, P. C., Yu, H. G., Mistrot, C., Unal, E., Koshland, D. E., DeRisi, J. L., and Gerton, J. L. (2004). Genome-wide mapping of the cohesin complex in the yeast Saccharomyces cerevisiae. *PLoS biology, 2*(9), e259.

Gustafsson, M. G. L., Shao, L., Carlton, P. M., Wang, R. C. J., Golubovskaya, I. N., Cande, W. Z., Agard, D. A., and Sedat, J. W. (2008). Three-dimensional resolution doubling in wide-field fluorescence microscopy by structured illumination. *Biophys J, 94*(12), 4957–4970.

Hawley, R. S. (2011). Solving a Meiotic LEGO¥textsuperscript®¥ Puzzle: Transverse Filaments and the Assembly of the Synaptonemal Complex in ¥textitCaenorhabditis elegans. *Genetics, 189*(2), 405–409.

Hayashi, M., Mlynarczyk-Evans, S., and Villeneuve, A. M. (2010). The Synaptonemal Complex Shapes the Crossover Landscape Through Cooperative Assembly, Crossover Promotion and Crossover Inhibition During *Caenorhabditis elegans* Meiosis. *Genetics,186(1), 45-58.*

Hess, H. (2010). iPALM: 3D Optical Imaging of Protein Locations at the Nanometer Level. *Biophysical Journal, 98*, 619.

Higgins, J. D., Sanchez-Moran, E., Armstrong, S. J., Jones, G. H., and Franklin, F. C. H. (2005). The Arabidopsis synaptonemal complex protein ZYP1 is required for chromosome synapsis and normal fidelity of crossing over. *Genes Dev., 19*(20), 2488–2500.

Hiraoka, Y. and Dernburg, A. F. (2009). The SUN rises on meiotic chromosome dynamics. *Developmental cell, 17*(5), 598–605.

Huang, B., Wang, W., Bates, M., and Zhuang, X. (2008). Three-dimensional super-resolution imaging by stochastic optical reconstruction microscopy. *Science, 319*(5864), 810-3.

Ishiguro, K. I., Kim, J., Fujiyama-Nakamura, S., Kato, S., and Watanabe, Y. (2011). A new meiosis-specific cohesin complex implicated in the cohesin code for homologous pairing. *EMBO Rep,12(3),267—275.*

Juette, M. F., Gould, T. J., Lessard, M. D., Mlodzianoski, M. J., Nagpure, B. S., Bennett, B. T., Hess, S. T., and Bewersdorf, J. (2008). Three-dimensional sub-100 nm resolution fluorescence microscopy of thick samples. *Nat Methods, 5*(6), 527-9.

Kleckner, N. (2006). Chiasma formation: chromatin/axis interplay and the role(s) of the synaptonemal complex. *Chromosoma, 115*(3), 175-94.

Kleckner, N., Zickler, D., Jones, G. H., Dekker, J., Padmore, R., Henle, J., and Hutchinson, J. (2004). A mechanical basis for chromosome function. *Proc Natl Acad Sci U S A, 101*(34), 12592-7.

Koszul, R., Kim, K. P., Prentiss, M., Kleckner, N., and Kameoka, S. (2008). Meiotic chromosomes move by linkage to dynamic actin cables with transduction of force through the nuclear envelope. *Cell, 133*(7), 1188-201.

Lee, J. and Hirano, T. (2011). RAD21L, a novel cohesin subunit implicated in linking homologous chromosomes in mammalian meiosis. *J Cell Biol, 192*(2), 263-76.

Lin, Y. (1979). Fine structure of meiotic prophase chromosomes and modified synaptonemal complexes in diploid and triploid Rhoeo spathacea. *Journal of Cell Science, 37*(1), 69.

MacQueen, A. J., Colaiacovo, M. P., McDonald, K., and Villeneuve, A. M. (2002, Sep). Synapsis-dependent and -independent mechanisms stabilize homolog pairing during meiotic prophase in C. elegans. *Genes Dev, 16*(18), 2428–2442.

Marko, J. F. and Siggia, E. D. (1997). Polymer models of meiotic and mitotic chromosomes. *Mol Biol Cell, 8*(11), 2217–2231.

Møens, P. B. and Pearlman, R. E. (1988). Chromatin organization at meiosis. *BioEssays, 9*(5), 151–153.

Morimoto, A., Shibuya, H., Zhu, X., Kim, J., Ishiguro, K.-i., Han, M., and Watanabe, Y. (2012). A conserved KASH domain protein associates with telomeres, SUN1, and dynactin during mammalian meiosis. *J Cell Biol, 198*(2), 165-72.

Moses, M. J. (1956). Chromosomal structures in crayfish spermatocytes. *J Biophys Biochem Cytol, 2*(2), 215-8.

Moses, M. and Poorman, P. (1981). Synaptonemal complex analysis of mouse chromosomal rearrangements. *Chromosoma, 81*(4), 519–535.

Moses, M., Poorman, P., Roderick, T., and Davisson, M. (1982). Synaptonemal complex analysis of mouse chromosomal rearrangements. *Chromosoma, 84*(4), 457–474.

Page, S. L., Khetani, R. S., Lake, C. M., Nielsen, R. J., Jeffress, J. K., Warren, W. D., Bickel, S. E., and Hawley, R. S. (2008). Corona is required for higher-order assembly of transverse filaments into full-length synaptonemal complex in Drosophila oocytes. *PLoS Genet, 4*(9), e1000194.

Phillips, D., Nibau, C., Wnetrzak, J., and Jenkins, G. (2012). High Resolution Analysis of Meiotic Chromosome Structure and Behaviour in Barley (Hordeum vulgare L.). *PLoS One, 7*(6), e39539.

This study employed 3D-SIM to characterize synaptonemal complex formation and structure in barley. The authors discovered that a two-level organization of the central element exists in addition to the canonical one-level structure.

Poorman, P., Moses, M., Russell, L., and Cacheiro, N. (1981). Synaptonemal complex analysis of mouse chromosomal rearrangements. *Chromosoma, 81*(4), 507–518.

Qiao, H., Chen, J. K., Reynolds, A., Höög, C., Paddy, M., and Hunter, N. (2012). Interplay between Synaptonemal Complex, Homologous Recombination, and Centromeres during Mammalian Meiosis. *PLoS Genet, 8*(6), e1002790.

The synaptonemal complex in mouse spermatocytes was characterized with 3D-SIM. Central element protein Sycp1 was found to persist at centromeres and at sites of crossing-over, despite being removed normally from the rest of the chromosome. Abnormal axis morphology in the absence of Sycp1 protein suggested a role of these persistent SC fragments in maintaining axis integrity and preventing abnormal axis association.

Rasmussen, S. W. (1977). Chromosome pairing in triploid females of Bombyx mori analyzed by three dimensional reconstructions of synaptonemal complexes. *Carlsberg Research Communications, 42*(3), 163–197.

Rasmussen, S. W. and Holm, P. B. (1979). Chromosome pairing in autotetraploid Bombyx females. Mechanism for exclusive bivalent formation. *Carlsberg Research Communications, 44*(2), 101–125.

Rockmill, B., Sym, M., Scherthan, H., and Roeder, G. S. (1995). Roles for two RecA homologs in promoting meiotic chromosome synapsis. *Genes Dev, 9*(21), 2684–2695.

Schermelleh, L., Carlton, P. M., Haase, S., Shao, L., Winoto, L., Kner, P., Burke, B., Cardoso, C. M., Agard, D. A., Gustafsson, M. G., Leonhardt, H., and Sedat, J. W. (2008). Subdiffraction Multicolor Imaging of the Nuclear Periphery with 3D Structured Illumination Microscopy. *Science, 320*(5881), 1332–1336.

Schermelleh, L., Heintzmann, R., and Leonhardt, H. (2010). A guide to super-resolution fluorescence microscopy. *J Cell Biol, 190*(2), 165-175.

Schild-Prüfert, K., Saito, T. T., Smolikov, S., Gu, Y., Hincapie, M., Hill, D. E., Vidal, M., McDonald, K., and Colaiacovo, M. P. (2011). Organization of the Synaptonemal Complex During Meiosis in *Caenorhabditis elegans*. *Genetics,189(2), 411-421.*

Schmekel, K., Skoglund, U., and Daneholt, B. (1993). The three-dimensional structure of the central region in a synaptonemal complex: a comparison between rat and two insect species, Drosophila melanogaster andBlaps cribrosa. *Chromosoma, 102*(10), 682–692.

Schmidt, R., Wurm, C. A., Punge, A., Egner, A., Jakobs, S., and Hell, S. W. (2009). Mitochondrial cristae revealed with focused light. *Nano Lett, 9*(6), 2508–2510.

Schrader, M., Bahlmann, K., Giese, G., and Hell, S. W. (1998). 4Pi-confocal imaging in fixed biological specimens. *Biophys J, 75*(4), 1659–1668.

Shtengel, G., Galbraith, J.A., Galbraith, C.G., Lippincott-Schwartz, J., Gillette, J.M., Manley, S., Sougrat, R., Waterman, C.M., Kanchanawong, P., Davidson, M.W., et al. (2009). Interferometric fluorescent super-resolution microscopy resolves 3D cellular ultrastructure. *Proc Natl Acad Sci U S A, 106*, 3125–3130.

Solari, A. J. and Moses, M. J. (1973). The structure of the central region in the synaptonemal complexes of hamster and cricket spermatocytes. *The Journal of cell biology, 56*(1), 145–152.

Solari, A. (1992). Equalization of Z and W axes in chicken and quail oocytes. *Cytogenetic and Genome Research, 59*(1), 52–56.

Tease, C. and Fisher, G. (1986). Further examination of the production-line hypothesis in mouse foetal oocytes. *Chromosoma, 93*(5), 447–452.

Toomre, D. and Bewersdorf, J. (2010, Nov). A new wave of cellular imaging. *Annu Rev Cell Dev Biol, 26*, 285–314.

Vaughan, J. C., Jia, S., and Zhuang, X. (2012). Ultrabright photoactivatable fluorophores created by reductive caging. *Nat Methods,*epub ahead of print.

Voelkel-Meiman, K., Moustafa, S. S., Lefrançois, P., Villeneuve, A. M., and Macqueen, A. J. (2012). Full-Length Synaptonemal Complex Grows Continuously during Meiotic Prophase in Budding Yeast. *PLoS Genet, 8*(10), e1002993.

This paper used an inducible fluorescent Zip1 construct to "pulse" cells arrested in prophase, and whose SCs were already completely formed, with newly synthesized SC that could be differentially detected. They found dynamic, continual incorporation of new Zip1 into the mature SC, demonstrating that the proteins of the central element undergo turnover and dynamic repositioning.

Wang, C.-J. R., Carlton, P. M., Golubovskaya, I. N., and Cande, W. Z. (2009). Interlock Formation and Coiling of Meiotic Chromosome Axes During Synapsis. *Genetics, 183*(3),905–915.

Watts, F. and Hoffmann, E. (2011). SUMO meets meiosis: An encounter at the synaptonemal complex: SUMO chains and sumoylated proteins suggest that heterogeneous and complex interactions lie at the centre of the synaptonemal complex. *Bioessays,*33(7), 529–537.

Wynne, D. J., Rog, O., Carlton, P. M., and Dernburg, A. F. (2012). Dynein-dependent processive chromosome motions promote homologous pairing in C. elegans meiosis. *The Journal of Cell Biology, 196*(1), 47-64.

Zhang, W., Miley, N., Zastrow, M. S., Macqueen, A. J., Sato, A., Nabeshima, K., Martinez-Perez, E., Mlynarczyk-Evans, S., Carlton, P. M., and Villeneuve, A. M. (2012). HAL-2 Promotes Homologous Pairing during Caenorhabditis elegans Meiosis by Antagonizing Inhibitory Effects of Synaptonemal Complex Precursors. *PLoS Genet, 8*(8), e1002880.

Zickler, D. and Kleckner, N. (1999). Meiotic chromosomes: integrating structure and function. *Annu Rev Genet, 33*, 603-754.

Figure 1

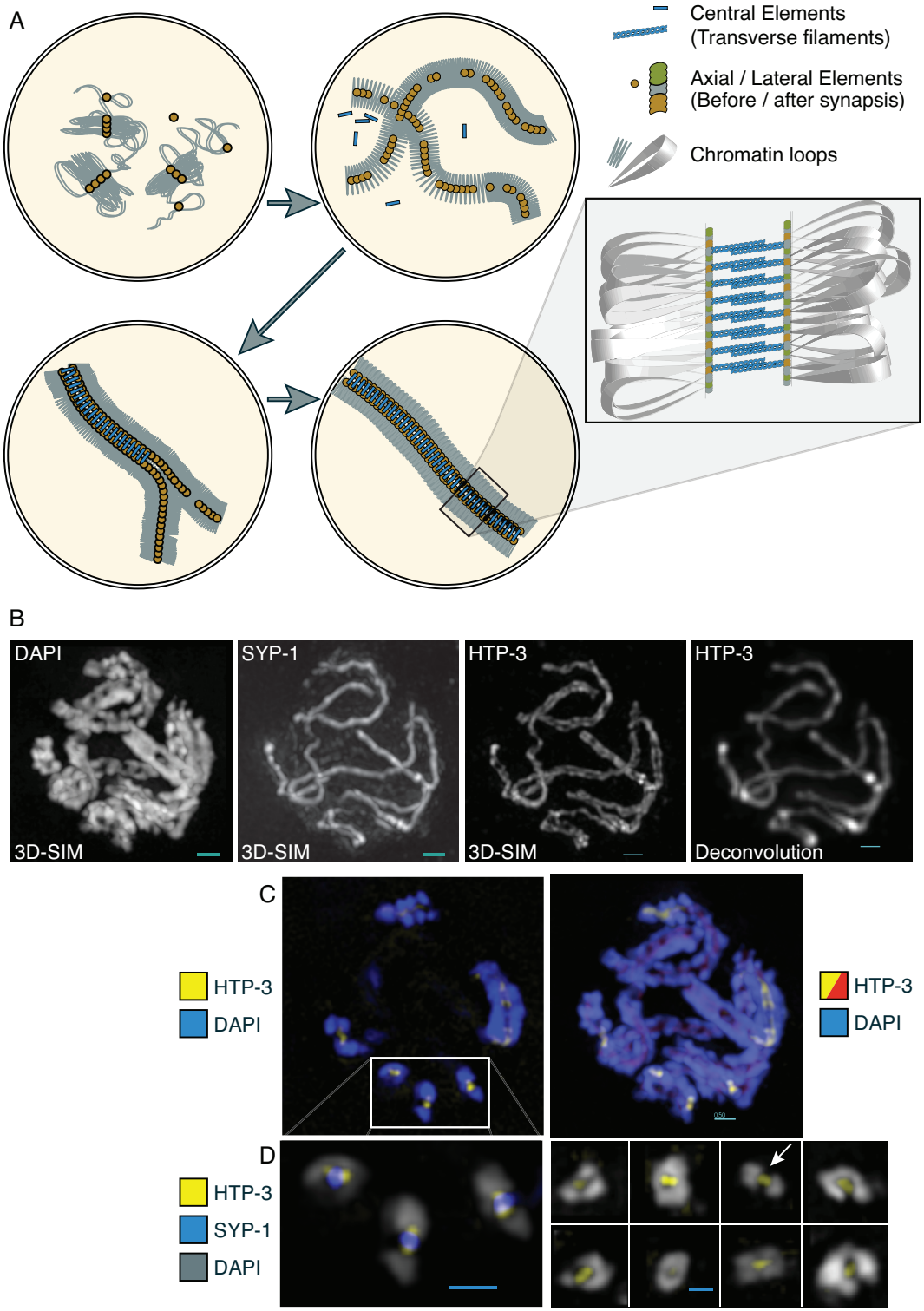
A
Central Elements
(Transverse filaments)
Axial / Lateral Elements
(Before / after synapsis)
Chromatin loops
B
DAPI
3D-SIM
SYP-1
3D-SIM
HTP-3
3D-SIM
HTP-3
Deconvolution
C
HTP-3
DAPI
HTP-3
DAPI
D
HTP-3
SYP-1
DAPI

Figure 2

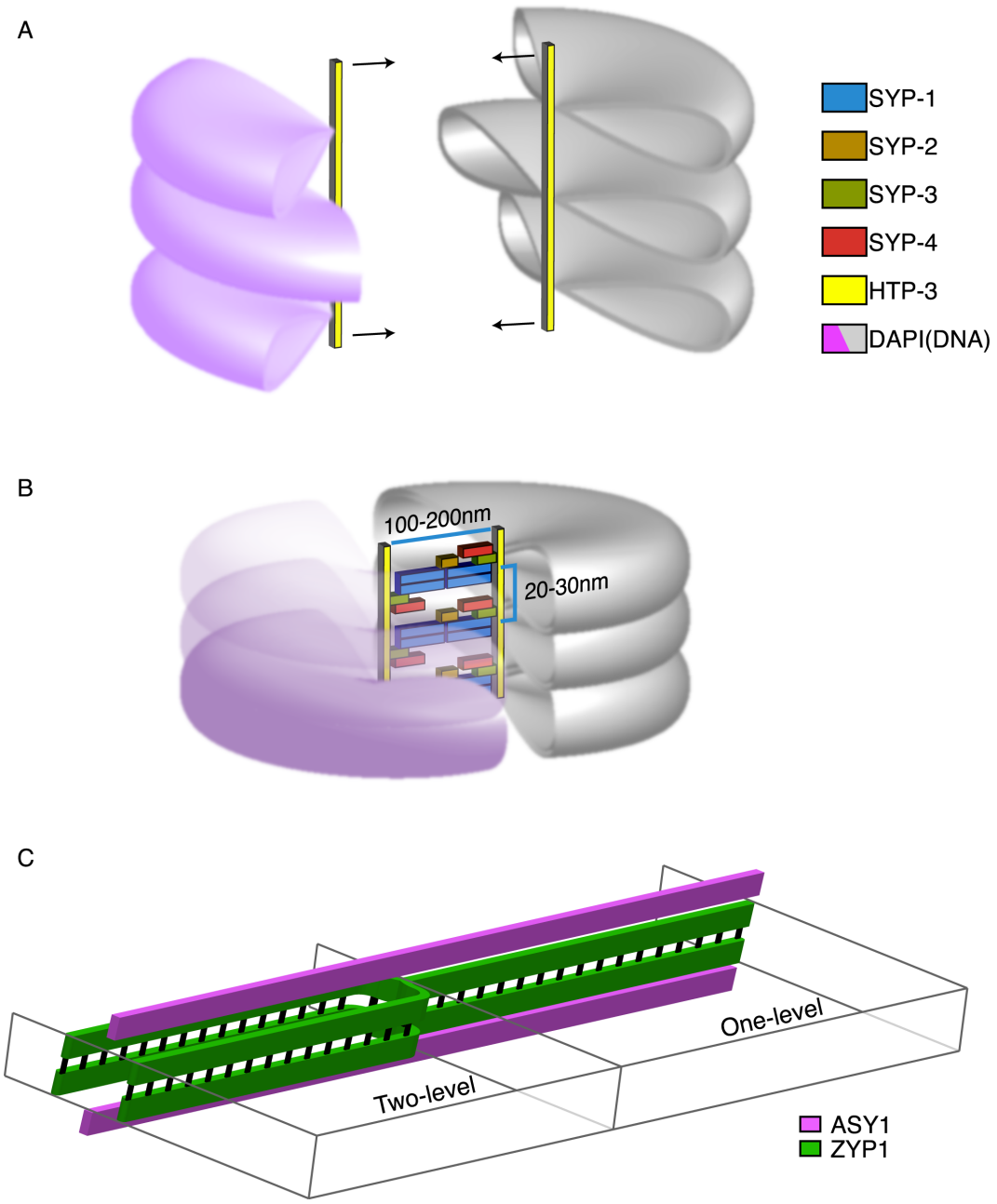
A
SYP-1
SYP-2
SYP-3
SYP-4
HTP-3
DAPI(DNA)
B
100-200nm
20-30nm
C
One-level
Two-level
ASY1
ZYP1

Figure 3